Half-metallic Transition Metal Oxides

Z. Szotek

Daresbury Laboratory, UK

Plan

1. Introduction – concepts and systems

2. SIC-LSD formalism

3. Results:

   a. Fe_3O_4
   b. double perovskites
   c. vacancy doped transition metal monoxides

4. Conclusions

Half Metals

(Half Metallic Ferromagnets)

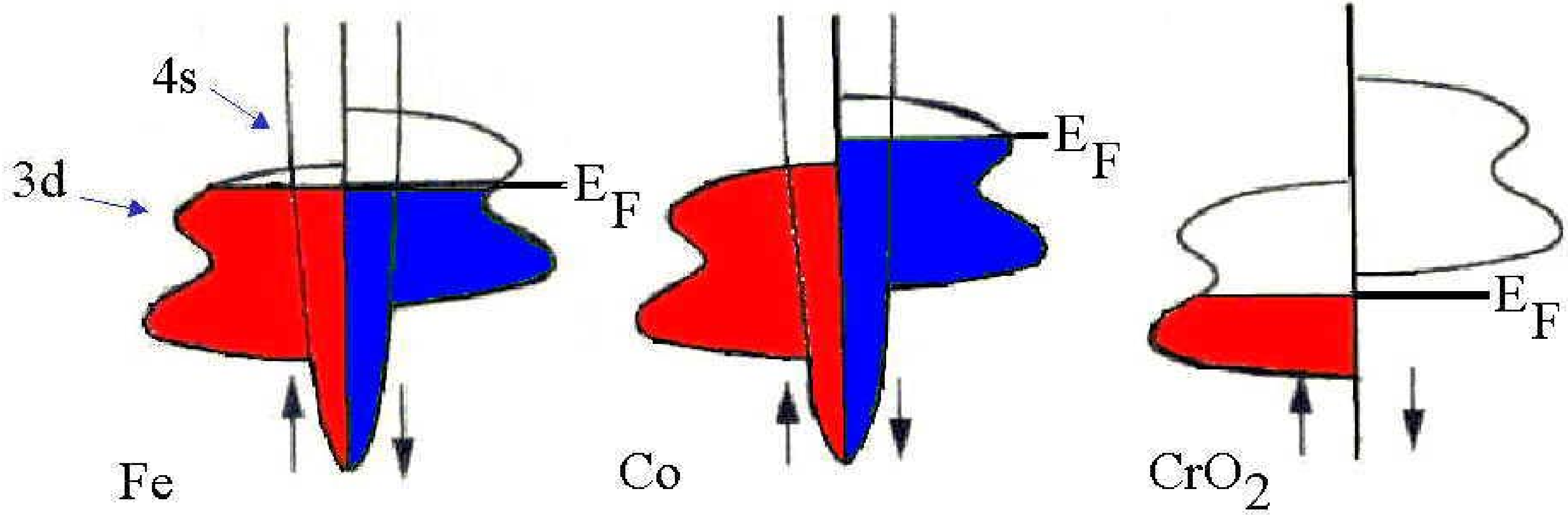

Half metals are ferromagnets whose density of states shows only one occupied spin-polarized sub-band at the Fermi energy E_F. Normal ferromagnets, like Fe and Co, have not only spin-polarized 3d electrons but also unpolarized 4s electrons at E_F. Half metals are compounds of more than one element and are mostly oxides or Heusler alloys.

CrO_2

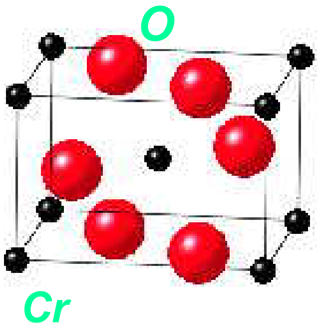

Chromium dioxide is the only simple oxide that is a ferromagnetic metal. Its resistivity increases rapidly as the temperature approaches the Curie point (T_C=398K)

Fe_3O_4

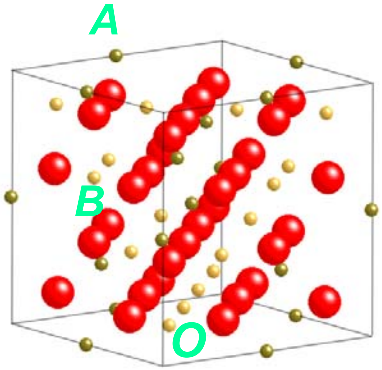

The oldest magnetic material known to man, Fe_3O_4 is also the half-metal with the highest Curie temperature of 860K.

Double Perovskites

Mixed Valence Manganites

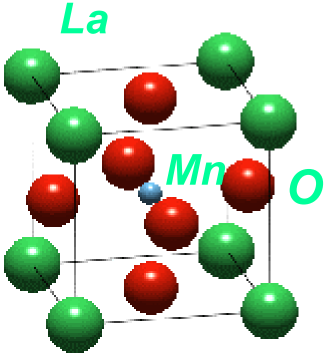

T_C of mixed-valence manganites cannot be increased above 400K.

$La_{(1-x)}A_xMnO_3$, A=Ca, Ba, Sr, x~0.3
(Poster by G. Banach, DL)

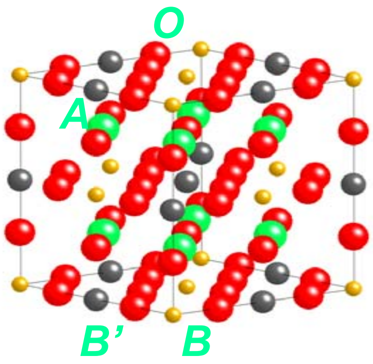

Double Perovskites such as Sr_2FeMoO_6 and Sr_2FeReO_6 are claimed to be half metals with T_C higher than 400K.

$A_2BB'O_6$, A=Ca, Sr, Ba
B – 3d transition metal (Fe, Co)
B' – 4d transition metal (Mo, Re)

Useful Properties

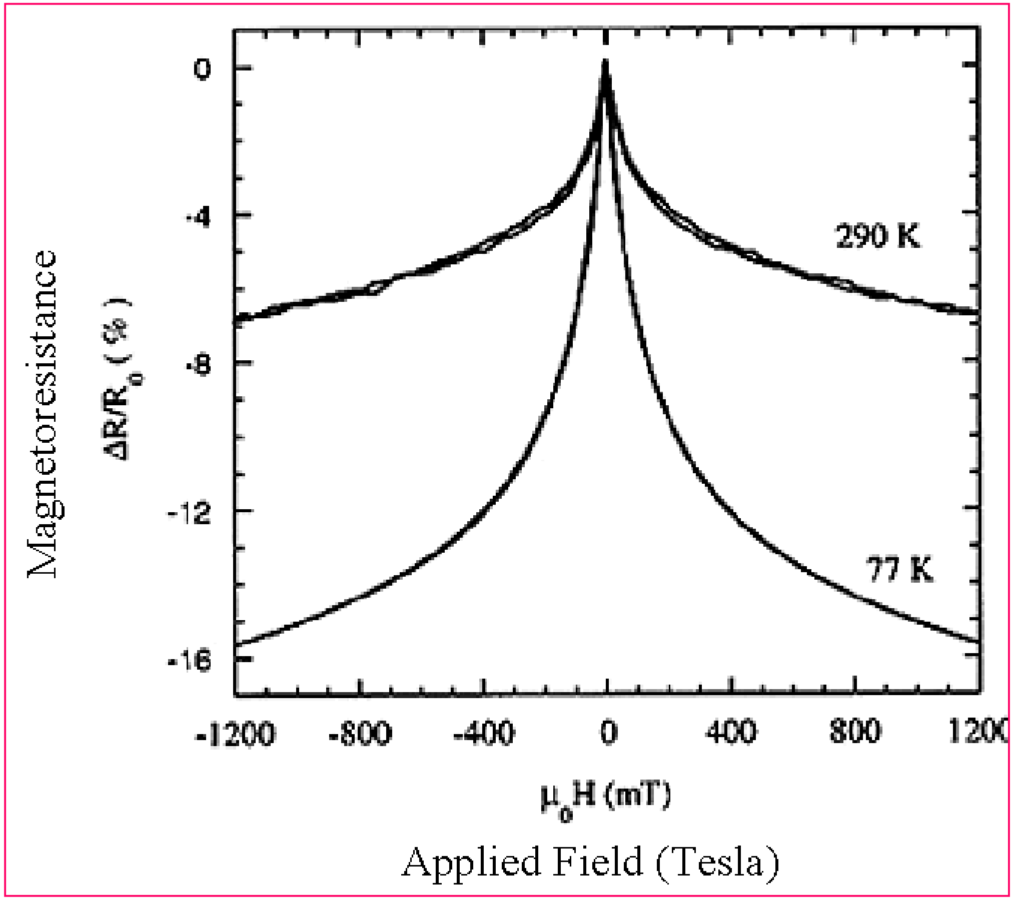

Half metallic ferromagnets
*-give rise to **100% spin polarization***
*-exhibit **colossal magnetoresistance** which can be usefully exploited in **magnetoresistive devices**.*
They can exploit the intrinisc magnetoresistance which arises from a polycrystalline grain structure.

Magnetoresistance of a ceramic sample of Sr_2FeMoO_6 made by a novel combustion synthesis procedure.

(R.P. Borges et al., J. Phys.: CM 11 (1999) L445-L450.)

Evidence for Half Metallic Behaviour

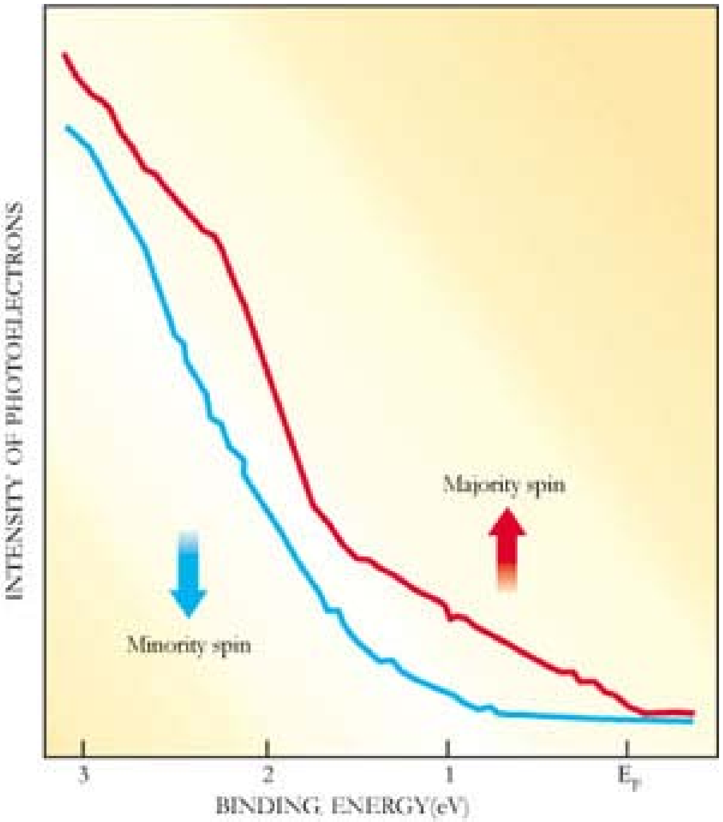

The measured photoelectron emission spectra of spin-up and spin-down electrons from the surface of a thin film of La0.7Sr0.3MnO3. The spectra illustrate the lack of detectable spin-down photoelectrons at the Fermi level, or even a few tenths of an eV below. Such a result, which indicates metallic spin-up electrons but a gap in the spin-down spectrum, is expected for half metallic character. The result also requires that both the bulk and the surface of the system be half metallic (because both regions are probed in this photoemission experiment).
(Adapted from J.-H. Park et al., Nature, volume 392, page 794, 1998.)

- *Spin polarized positron annihilation (FS for one spin only)*
- *Measurement of magnetic moment*
- *Tunnelling of electrons*
- *Optical spectroscopy*

Self-Interaction-Corrected Local Spin Density (SIC-LSD)

$$E^{SIC\text{-}LSD}[n] = E^{LSD}[n] - \Sigma_a \delta_a [n_a]$$

$$\delta_a [n_a] = E^{XC(LSD)}[n_a] + E^{H}[n_a]$$

- Corrects Local-Spin-Density (LSD) for spurious self-interaction.
- Is sizeable for a localised electron, i.e. when an electron spends a long time on a particular site.
- It reduces to the LSD for delocalised electrons.

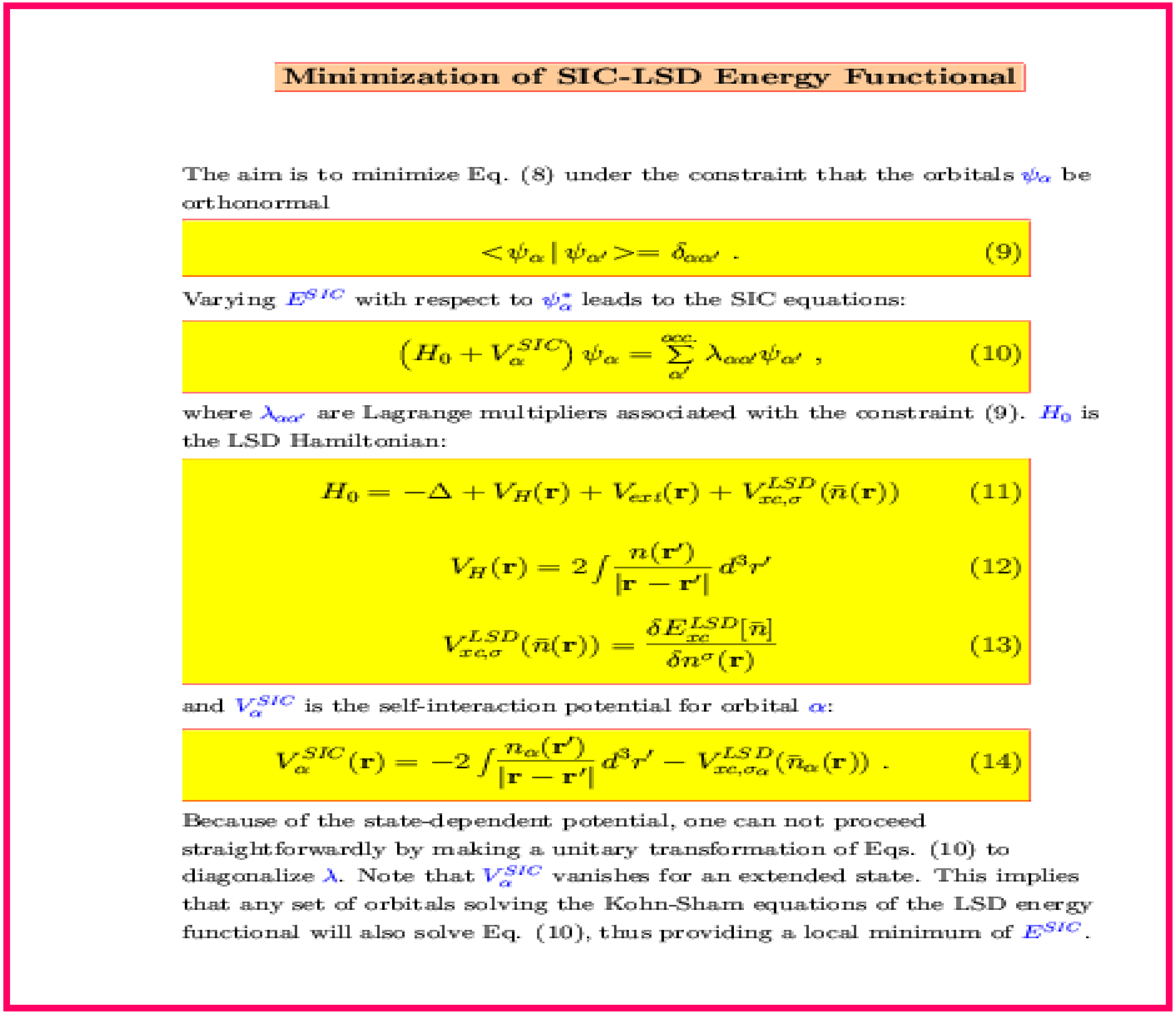

Minimization of SIC-LSD Energy Functional

The aim is to minimize Eq. (8) under the constraint that the orbitals ψ_α be orthonormal

$$<\psi_\alpha \,|\, \psi_{\alpha'}>= \delta_{\alpha\alpha'} \ . \tag{9}$$

Varying E^{SIC} with respect to ψ^*_α leads to the SIC equations:

$$\left(H_0 + V_\alpha^{SIC}\right)\psi_\alpha = \sum_{\alpha'}^{occ.} \lambda_{\alpha\alpha'}\psi_{\alpha'} \ , \tag{10}$$

where $\lambda_{\alpha\alpha'}$ are Lagrange multipliers associated with the constraint (9). H_0 is the LSD Hamiltonian:

$$H_0 = -\Delta + V_H(\mathbf{r}) + V_{ext}(\mathbf{r}) + V^{LSD}_{xc,\sigma}(\bar{n}(\mathbf{r})) \tag{11}$$

$$V_H(\mathbf{r}) = 2\int \frac{n(\mathbf{r}')}{|\mathbf{r}-\mathbf{r}'|}\, d^3r' \tag{12}$$

$$V^{LSD}_{xc,\sigma}(\bar{n}(\mathbf{r})) = \frac{\delta E^{LSD}_{xc}[\bar{n}]}{\delta n^\sigma(\mathbf{r})} \tag{13}$$

and V_α^{SIC} is the self-interaction potential for orbital α:

$$V_\alpha^{SIC}(\mathbf{r}) = -2\int \frac{n_\alpha(\mathbf{r}')}{|\mathbf{r}-\mathbf{r}'|}\, d^3r' - V^{LSD}_{xc,\sigma_\alpha}(\bar{n}_\alpha(\mathbf{r})) \ . \tag{14}$$

Because of the state-dependent potential, one can not proceed straightforwardly by making a unitary transformation of Eqs. (10) to diagonalize λ. Note that V_α^{SIC} vanishes for an extended state. This implies that any set of orbitals solving the Kohn-Sham equations of the LSD energy functional will also solve Eq. (10), thus providing a local minimum of E^{SIC}.

$$N_{val} = Z - N_{core} - N_{s\text{-}core} - N_{SIC}$$

Magnetite

Fe_3O_4 → a mixed valent compound

→ $FeO + Fe_2O_3$

→ $Fe^{2+} + O^{2-} + (2\,Fe^{3+} + 3O^{2-})$

→ The Verwey transition at 122 K

(monoclinic structure)

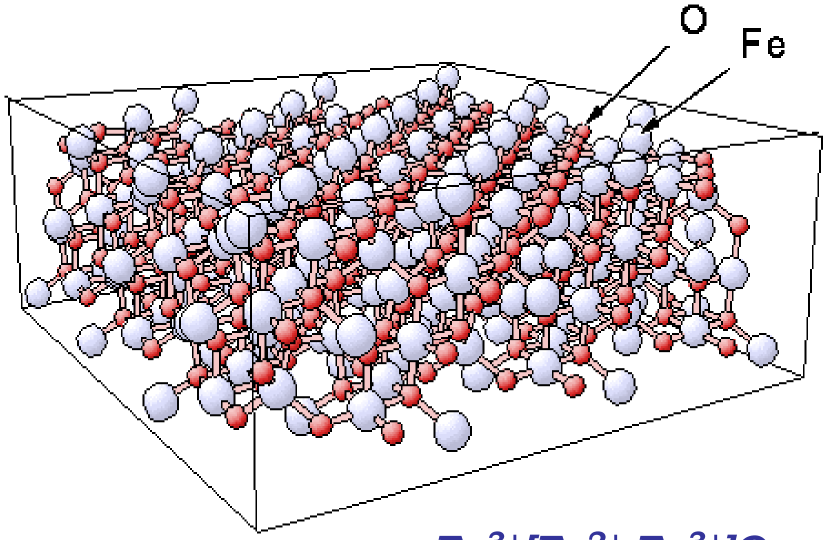

$Fe^{3+}[Fe^{2+}\,Fe^{3+}]O_4$

Fe_3O_4 (magnetite) lattice

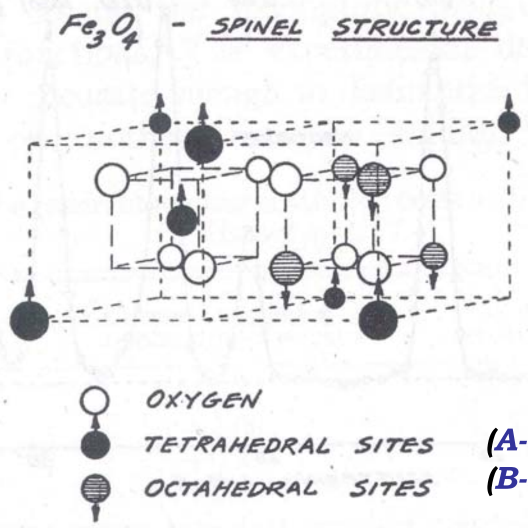

(inverse)

(A-sites)

(B-sites)

FIG. 5. Portion of the magnetic unit cell for Fe_3O_4. The octahedral and tetrahedral Fe ions are coupled antiferromagnetically.

A-sites are occupied by Fe^{3+}

B-sites are occupied by Fe^{3+} and Fe^{2+}

Shull, Wollan, Koehler, PR 84, 912 (1951)

Charge Order on Octahedral Sites in Fe_3O_4

Fe^{2+} (d^6)

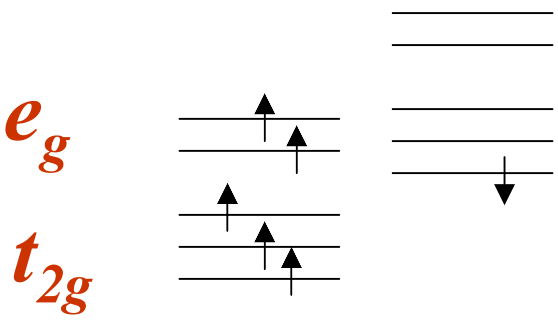

S=2

Fe^{3+} (d^5)

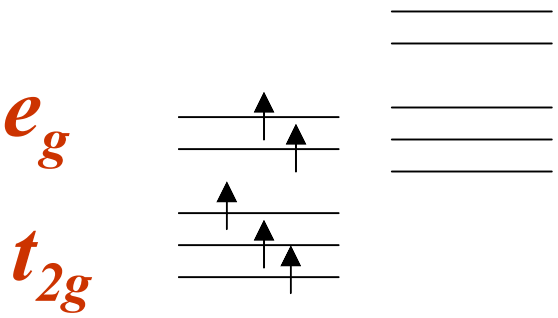

S=5/2

Configurations studied: Fe 3+ and Fe 2+ on alternating (001) planes
all octahedral Fe's to be 3+
all octahedral Fe's to be 2+

LSD **SIC-LSD**

Total DOS

Fe

O

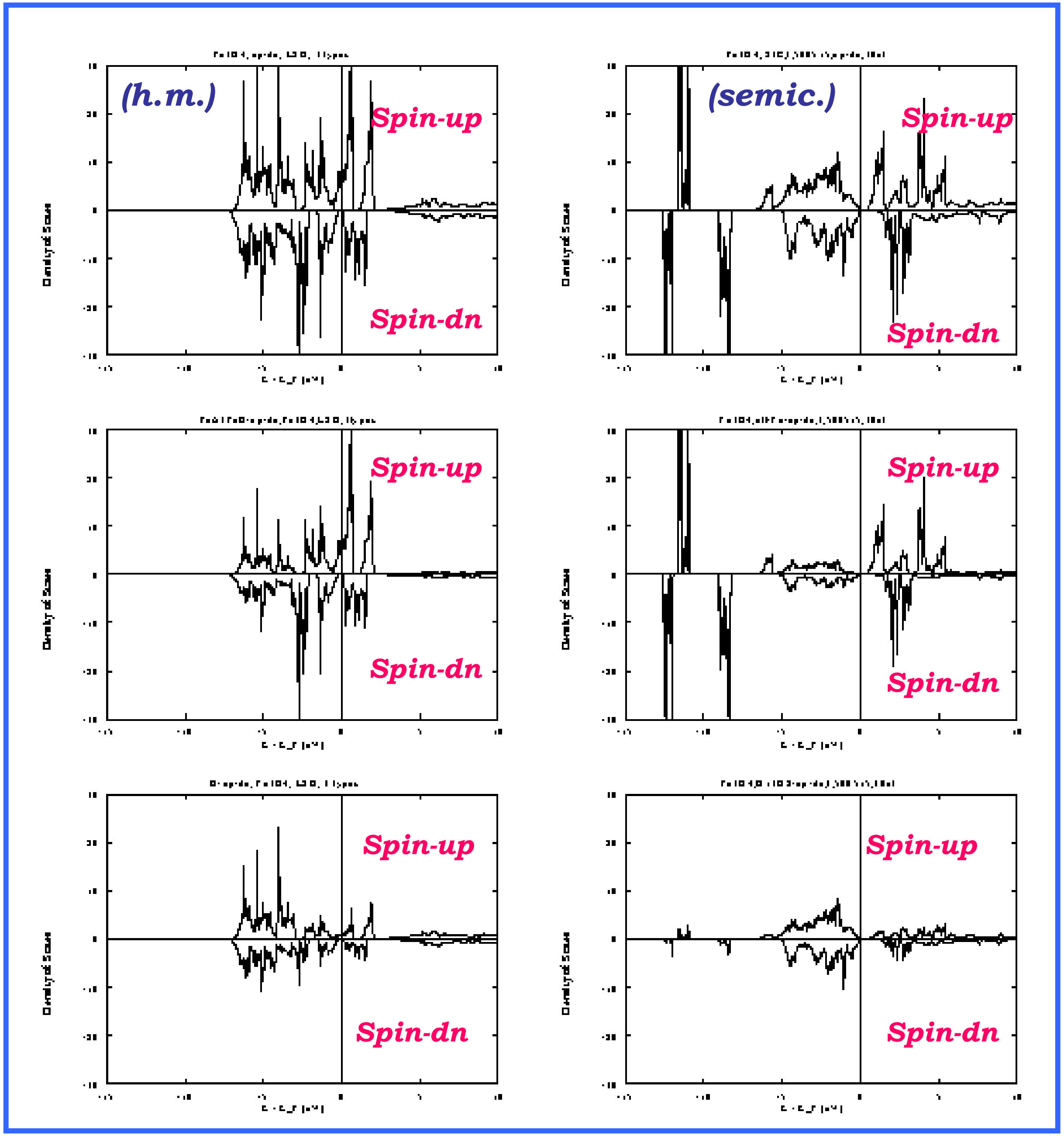

LSD **SIC-LSD**

Tetrahedral Sites

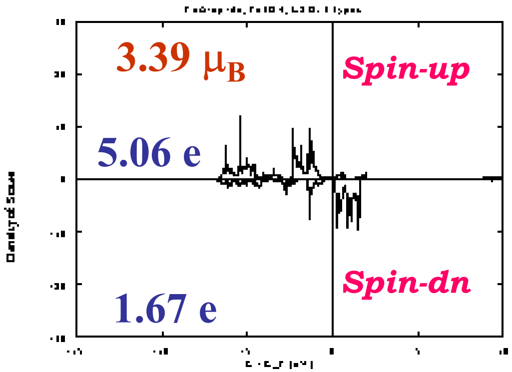

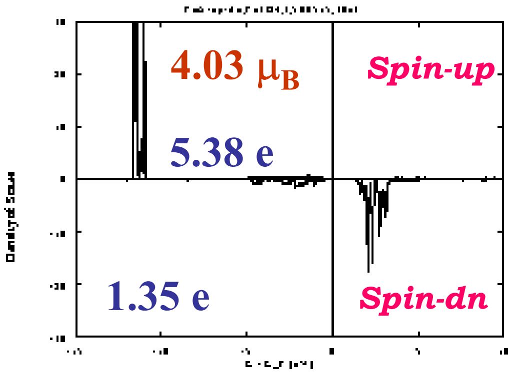

Fe^{3+}

Octahedral Sites

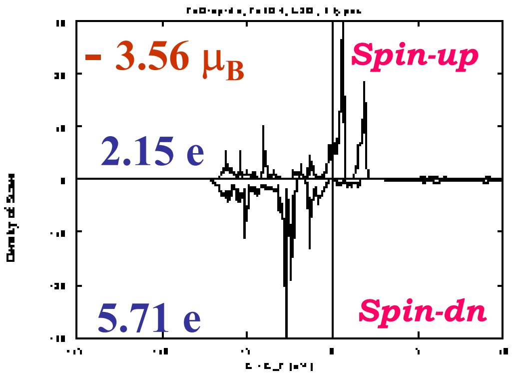

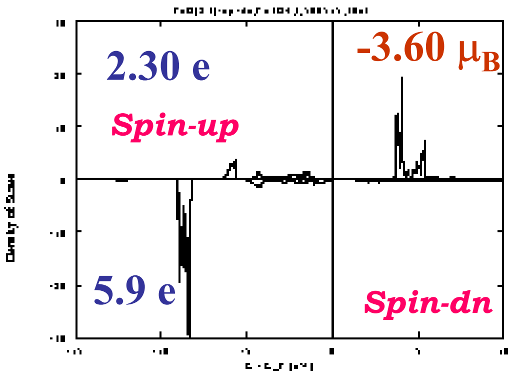

Fe^{2+}

$m_{tot} = 4.0\ \mu_B/f.u.$

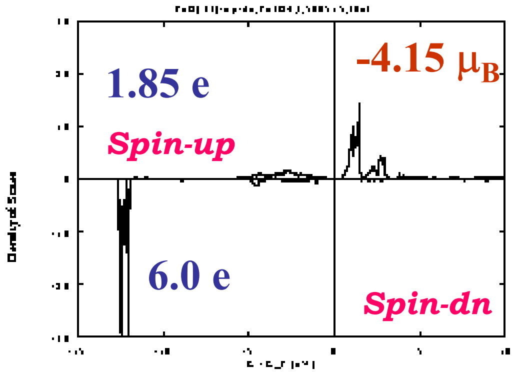

Fe^{3+}

Summary of Results for Fe_3O_4 (cubic)

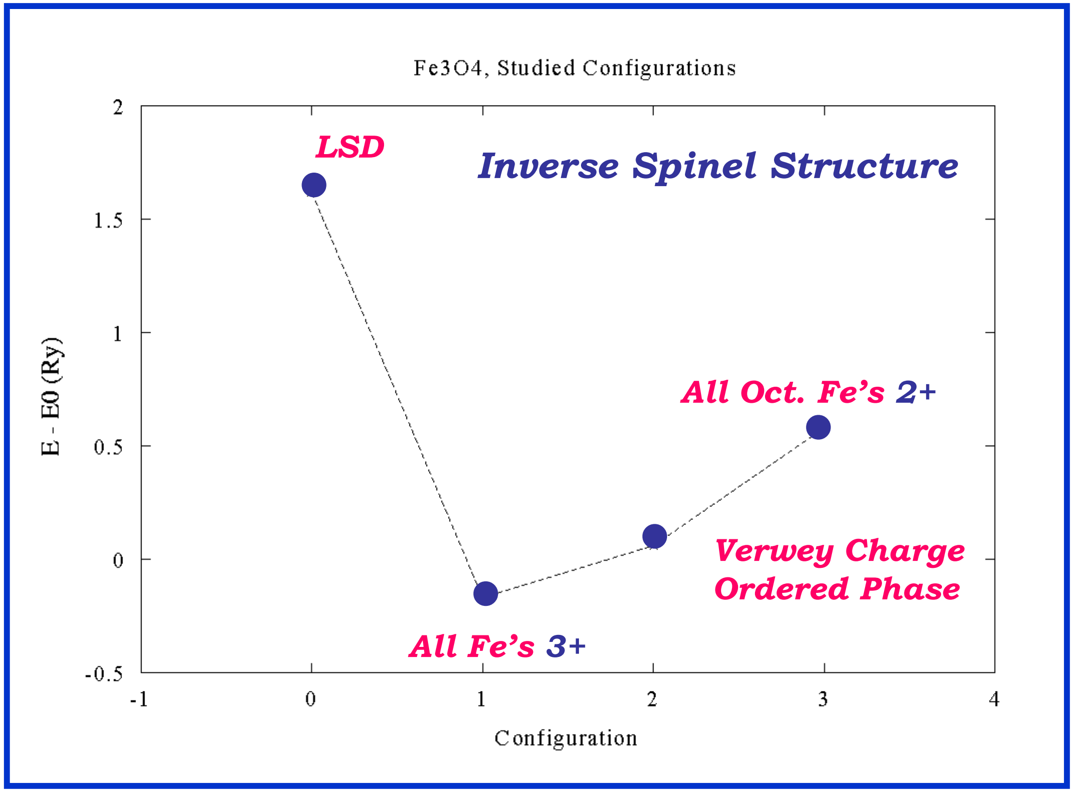

Config. 0: (h.m.)

$m_{tot} = 4.0\ \mu_B$

Config. 1: (h.m.)

$m_{tot} = 4.0\ \mu_B$

Config. 2: (semic.)

$m_{tot} = 4.0\ \mu_B$

gap = ~0.35 eV
gap_{exp} = 0.14 eV

Config. 3: (h.m.)

$m_{tot} = 2.0\ \mu_B$

Summary of Results for Fe_3O_4 (orthorombic)

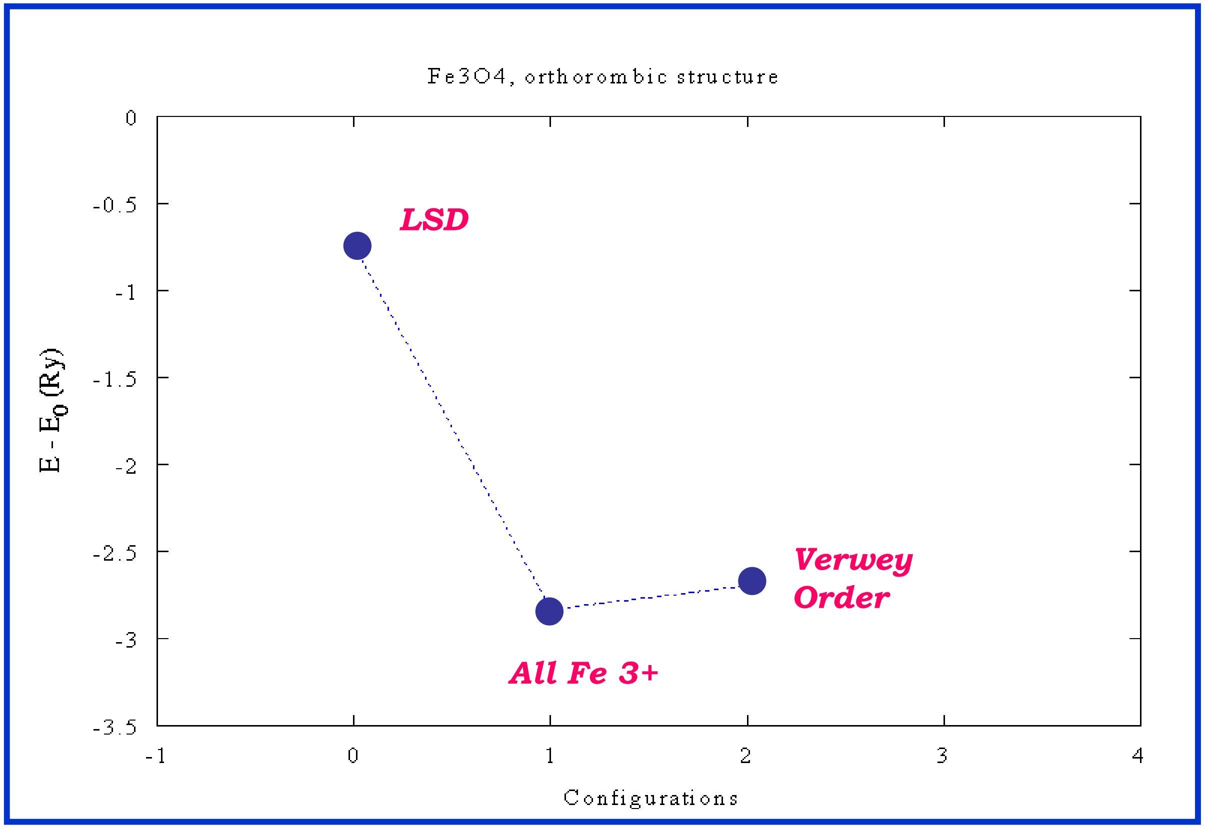

Config. 0: (h.m.)

$m_{tot} = 4.0\ \mu_B$

Config. 1: (metal)

$m_{tot} > 4.0\ \mu_B$

Config. 2: (semic.)

$m_{tot} = 4.0\ \mu_B$

Double Perovskites

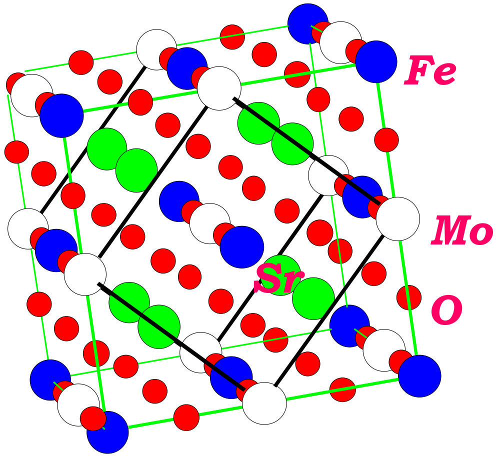

A_2FeMoO_6
A=Ba,Sr,Ca

Ba - cubic
Sr - tetragonal
Ca - monoclinic

Characteristics:

- -- *half-metallic behaviour*
- -- *metallic conductivity*
- -- *large Curie temperature*
- -- *intrinsic tunnelling-type magnetoresistance at room temperature and low field*

K.-I. Kobayashi et al., Nature 395, 677(1999)

ΔR/R (%)	Ca_2FeMoO_6	Sr_2FeMoO_6	Ba_2FeMoO_6
(at 77K, 1T, ceramic)	---	15.0%	13.5%
(at 290K, 50mT, ceramic)	---	2.6%	1.6%
(at 77K, 1T, pressed powder)	3.5%	6.0%	---
(at 290K, 50mT, pressed powder)	---	1.0%	
(at 4.2K, 7T, poly. ceramic)		42.0%	
(at 300K, 7T, poly. ceramic)		10.0%	

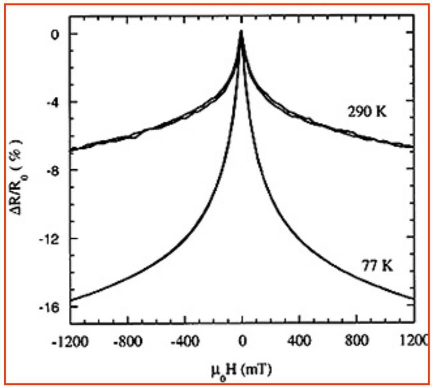

R.P. Borges et al., J. Phys.: CM 11 (1999) L445-L450.

Summary of Results for Perovskites

Moment (μ_B)	$Ca_2FeMo(Re)O_6$	Sr_2FeMoO_6	Ba_2FeMoO_6
M_{tot}	4.000 (3.000)	4.000	4.000
M_{Fe}	3.758 (3.872)	3.711 (3.645)	3.811
$M_{Mo\ (Re)}$	–0.404 (–1.124)	–0.425 (–0.349)	–0.414
$M_{(Ca,Sr,Ba)}$	0.005 (0.020)	0.021 (0.021)	0.020
M_{O1}	0.104 (0.019)	0.112 (0.112)	0.094
M_{O2}	0.107 (0.013)	0.113 (0.107)	---------
M_{O3}	0.108 (0.113)	--------	--------
Volume [$(au)^3$]	777.523 (773.823)	830.219	884.027

SIC-LSD Spin-resolved DOS

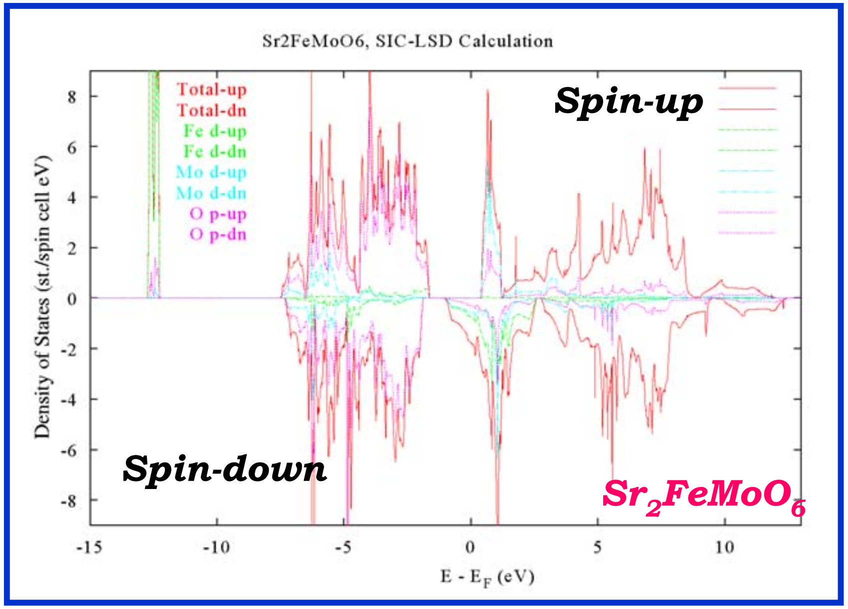

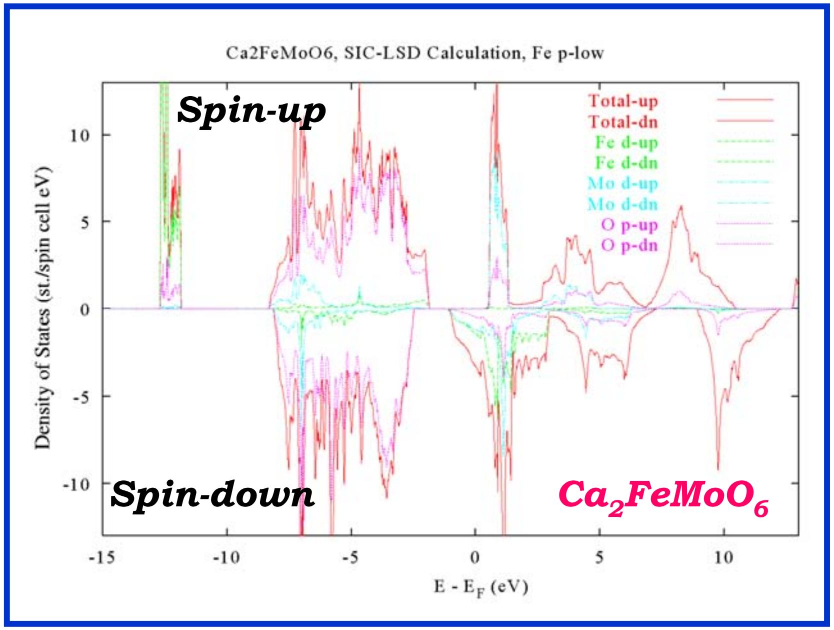

Sr_2FeMoO_6

$m_{Fe} = 3.711\ \mu_B$
$m_{Mo} = -0.425\ \mu_B$
$m_{O1} = 0.112\ \mu_B$
$m_{O2} = 0.113\ \mu_B$
$m_{Sr} = 0.021\ \mu_B$

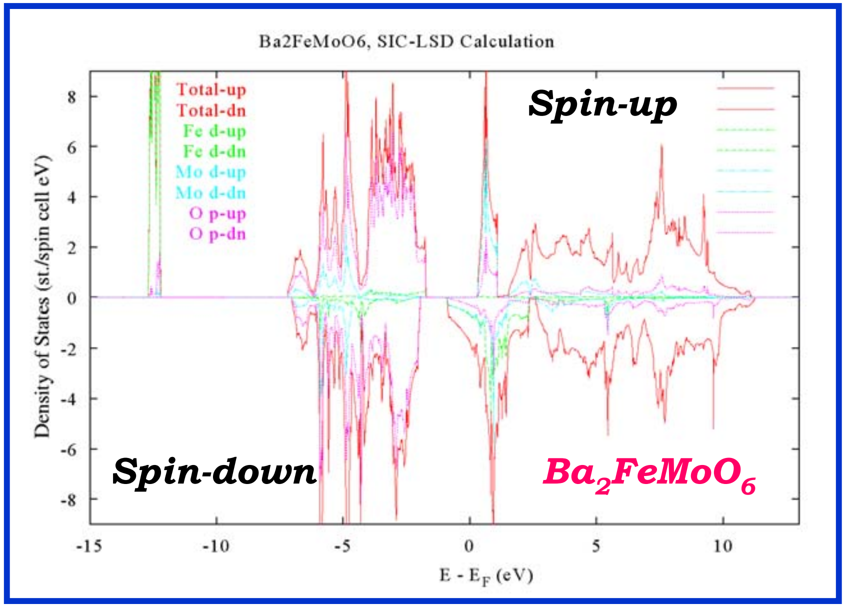

Ba_2FeMoO_6

$m_{Fe} = 3.811\ \mu_B$
$m_{Mo} = -0.414\ \mu_B$
$m_{O} = 0.094\ \mu_B$
$m_{Ba} = 0.020\ \mu_B$

Ca_2FeMoO_6

$m_{Fe} = 3.758\ \mu_B$
$m_{Mo} = -0.406\ \mu_B$
$m_{O1} = 0.104\ \mu_B$
$m_{O2} = 0.107\ \mu_B$
$m_{O3} = 0.108\ \mu_B$
$m_{Ca} = 0.005\ \mu_B$

Energy Considerations and Valency

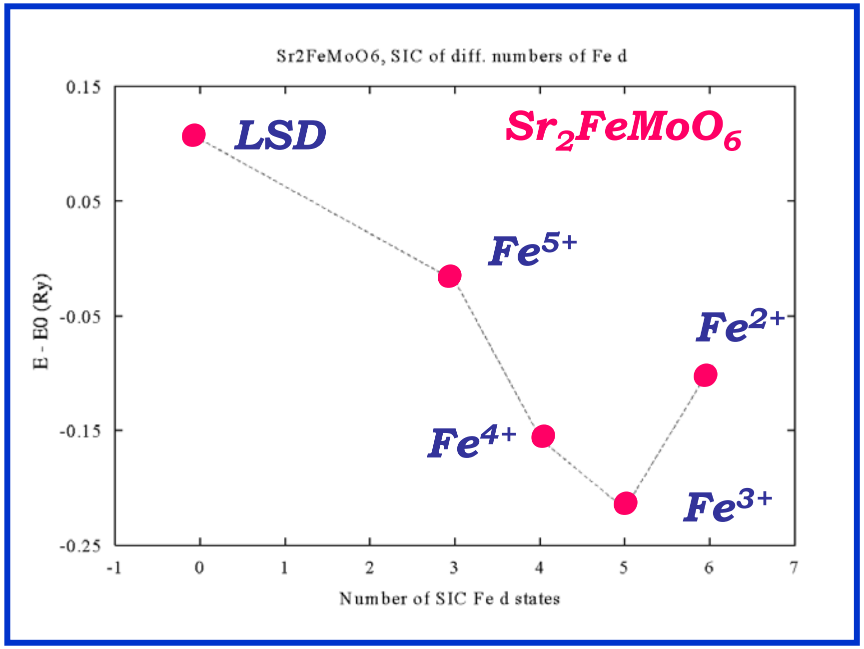

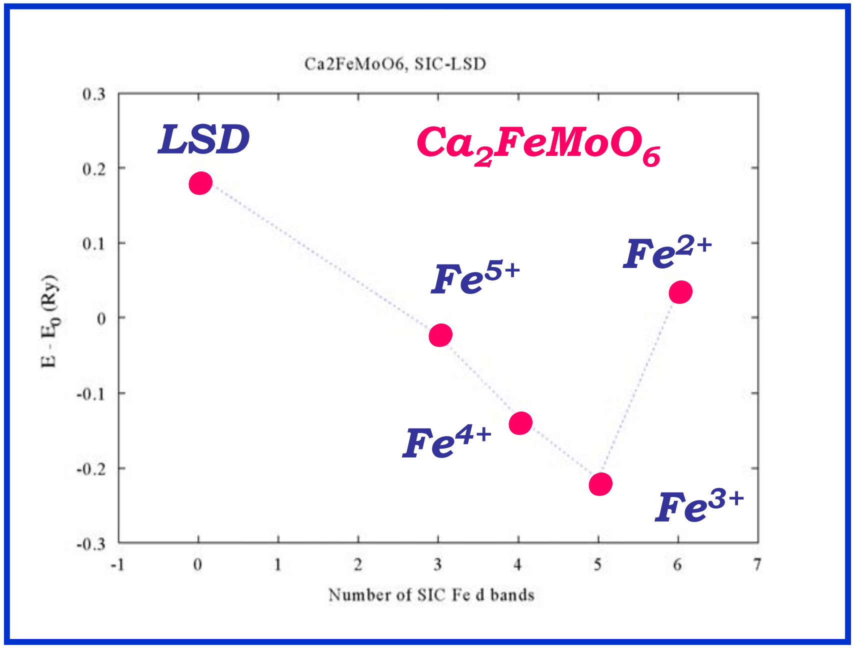

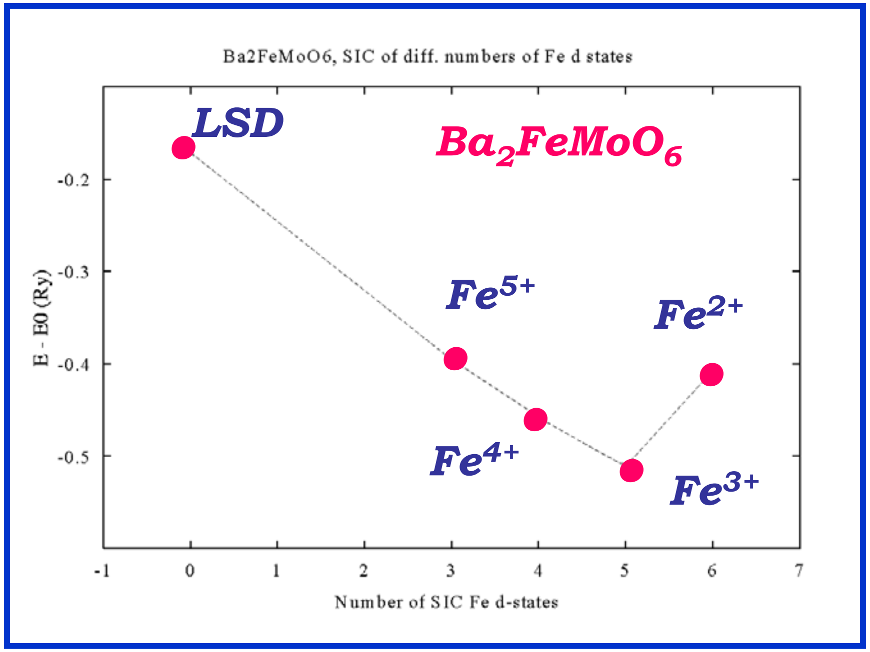

Fe^{3+} ($3d^5$) is the most favourable configuration (half-metallic). Fe^{2+} ($3d^6$) configuration is insulating.

Point Defect Induced Half-Metallicity in Transition Metal Oxides

- *Transition metal monoxides: point defect creation*

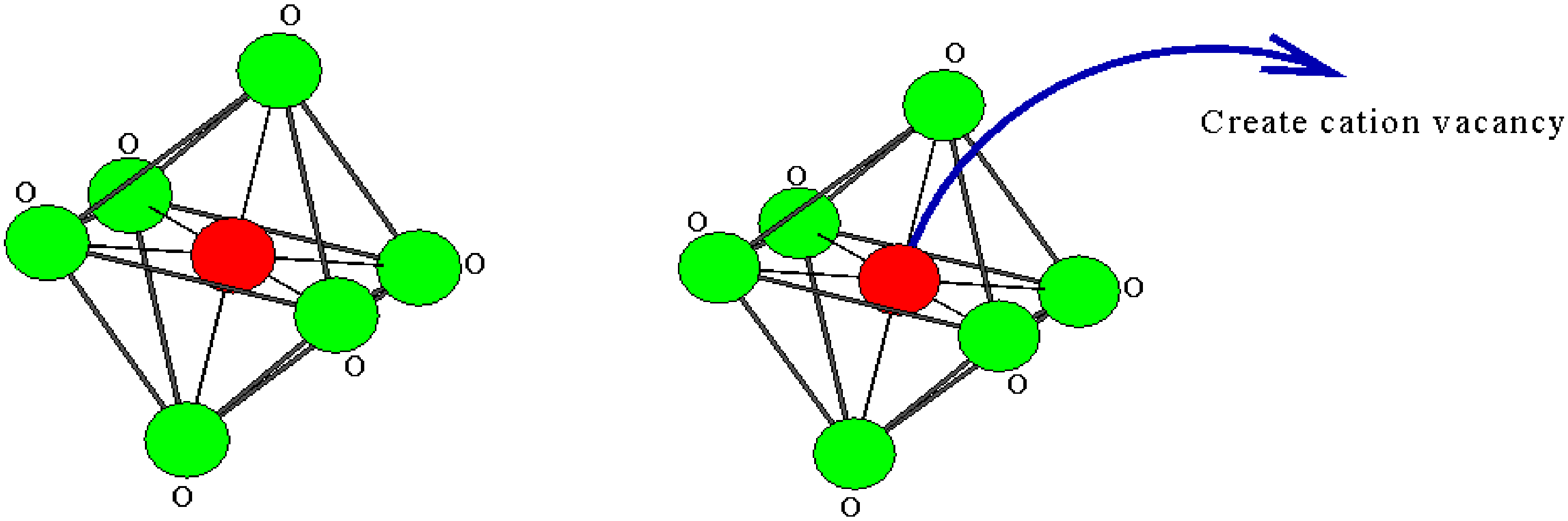

Cation site in octahedral coordination

(I.S. Elfimov et al., PRL 89, 216403 (2002); M.R. Castel et al., PRB 55, 7859 (1997).)

Super-cell Setup: NiO

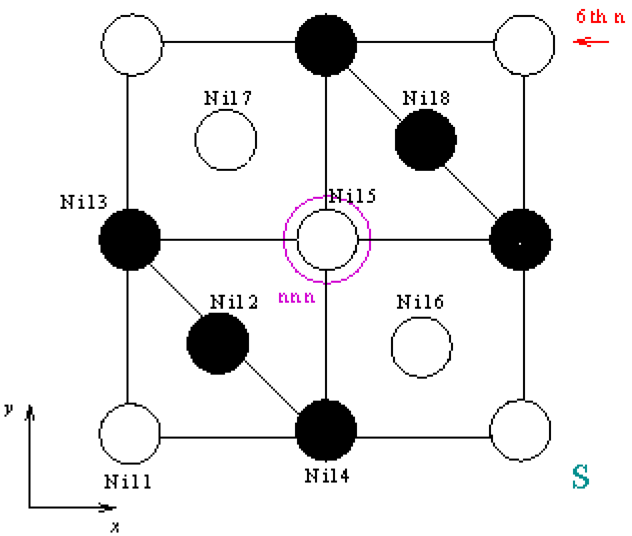

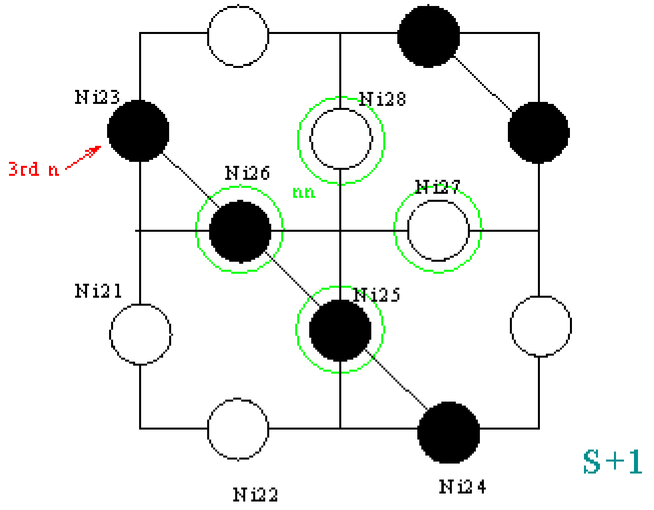

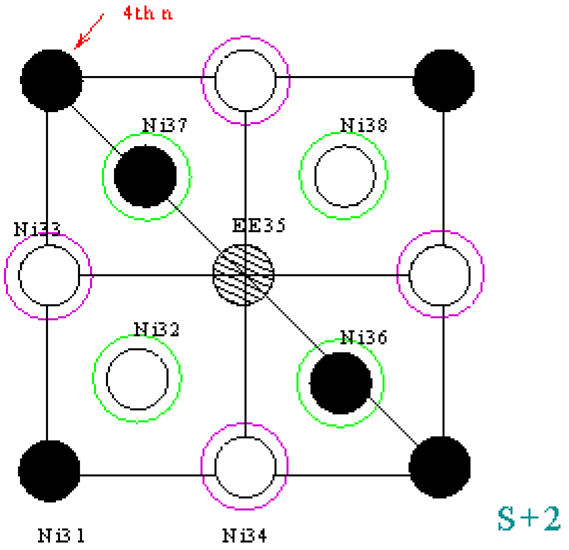

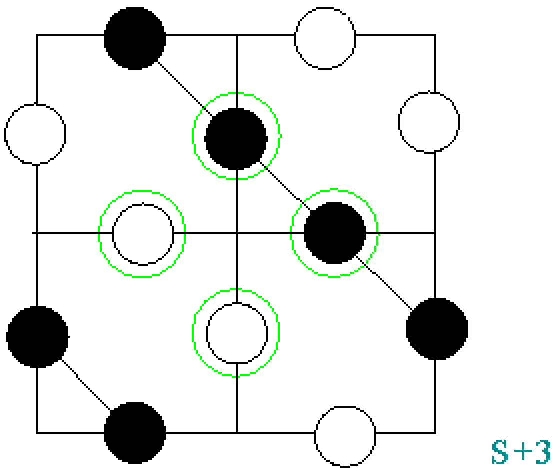

- 8 Ni per layer -> 31 Ni and one impurity
- O positions: add (0,0.5,0) to the Ni positions

3% vacancy doping realized

NiO in FM and AF2 arrangements

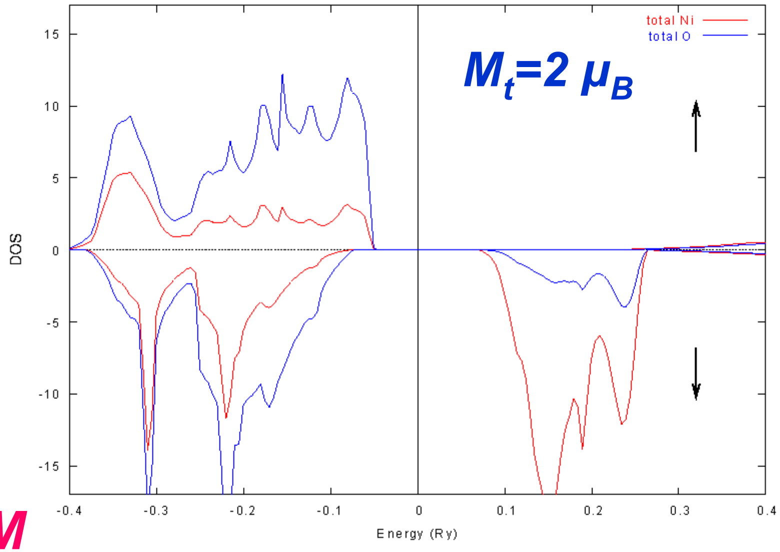

FM

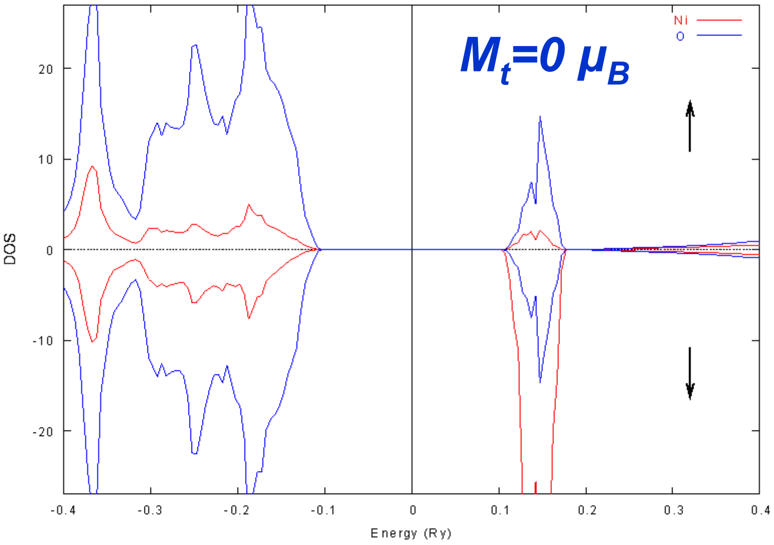

AFM

Insulator Half metal transition ([illegible]% vacancy doping)

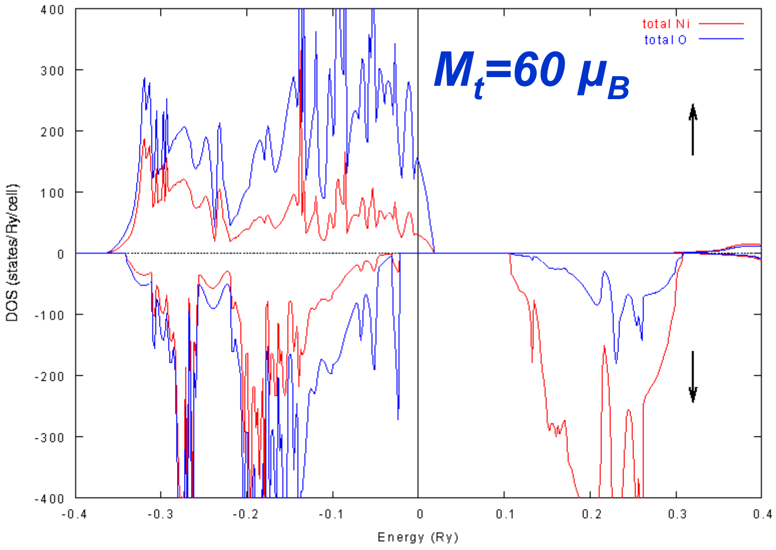

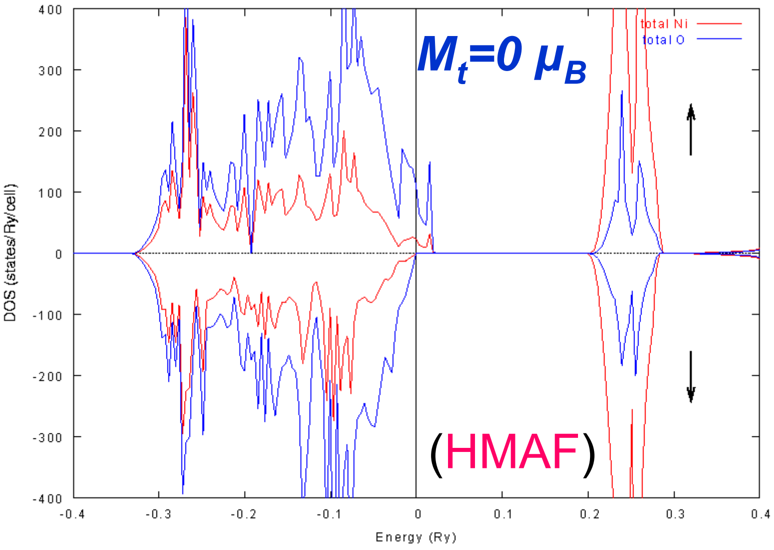

MnO in FM and AF2 arrangements

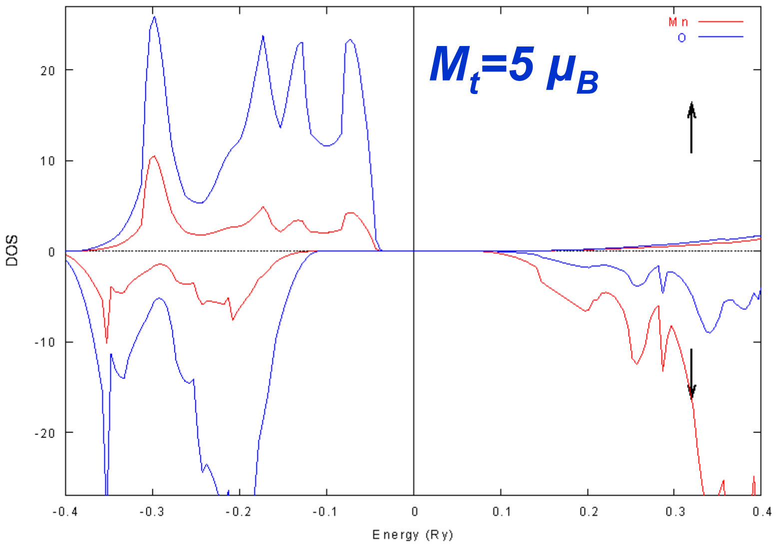

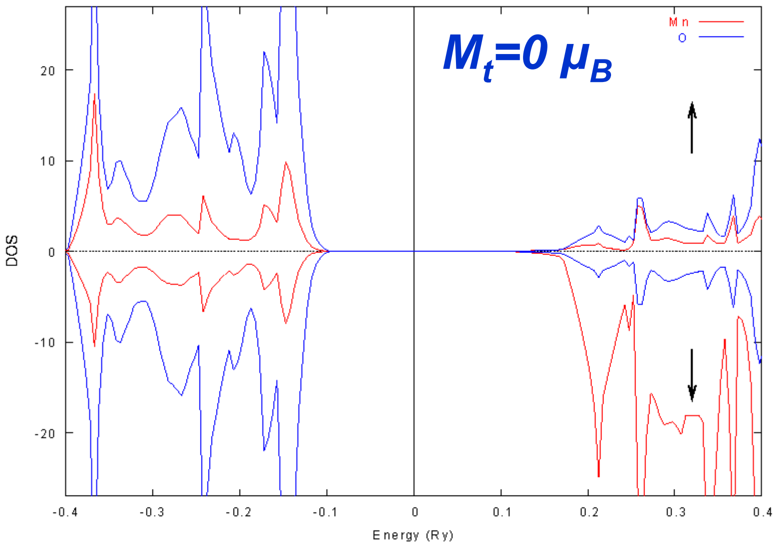

FM

AFM

Insulator → Half-metal transition (3% vacancy doping)

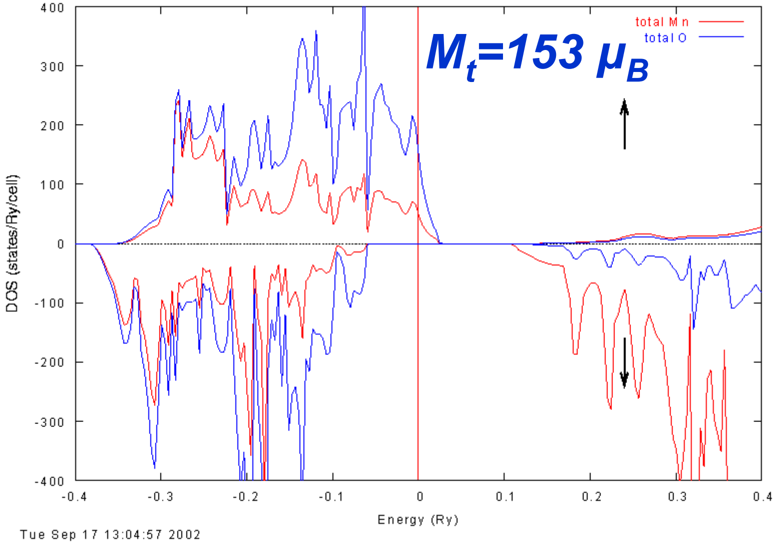

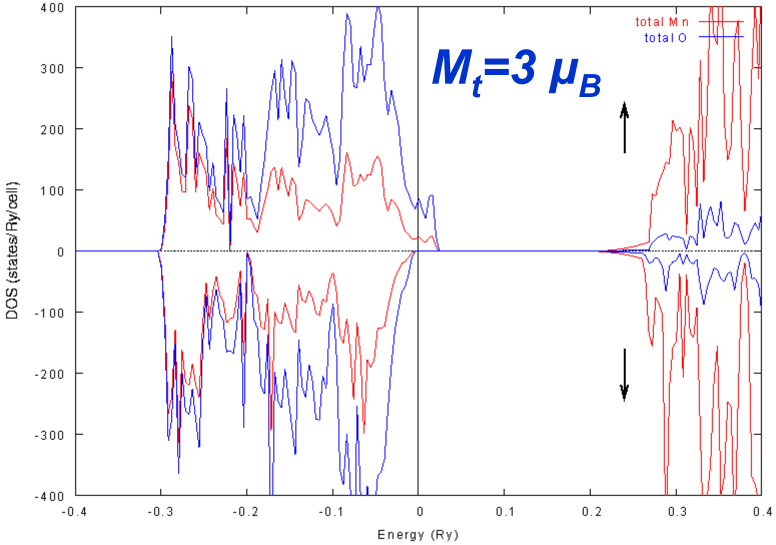

Distribution of magnetic moments around vacancy in the NiO super cell

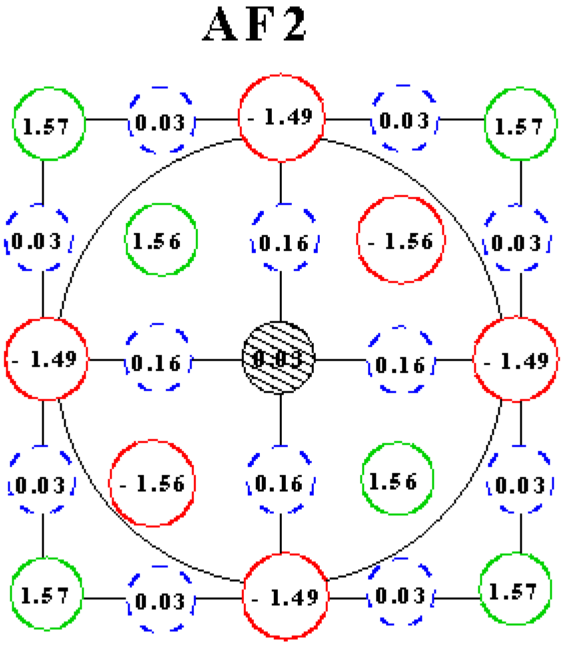

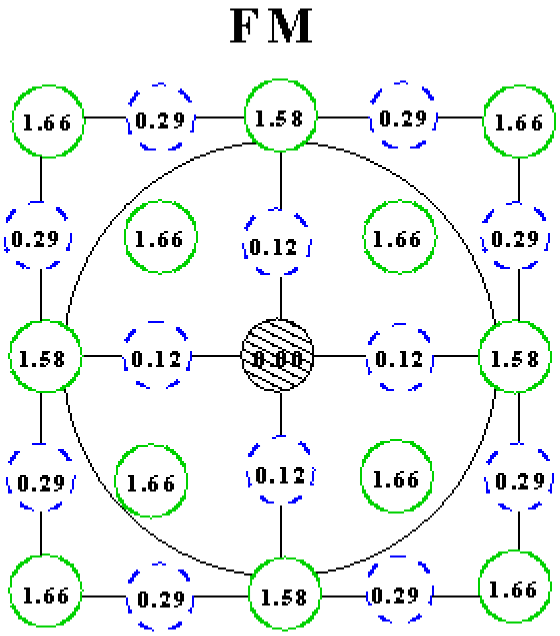

$M\ (Ni_{bulk}) = 1.57\ \mu_B$
$M\ (O_{bulk}) = 0.0\ \mu_B$

Green — **Ni-up**
Red — **Ni-down**
Blue — **Oxygen**

$M\ (Ni_{bulk}) = 1.66\ \mu_B$
$M\ (O_{bulk}) = 0.34\ \mu_B$

Total Magnetic Moments

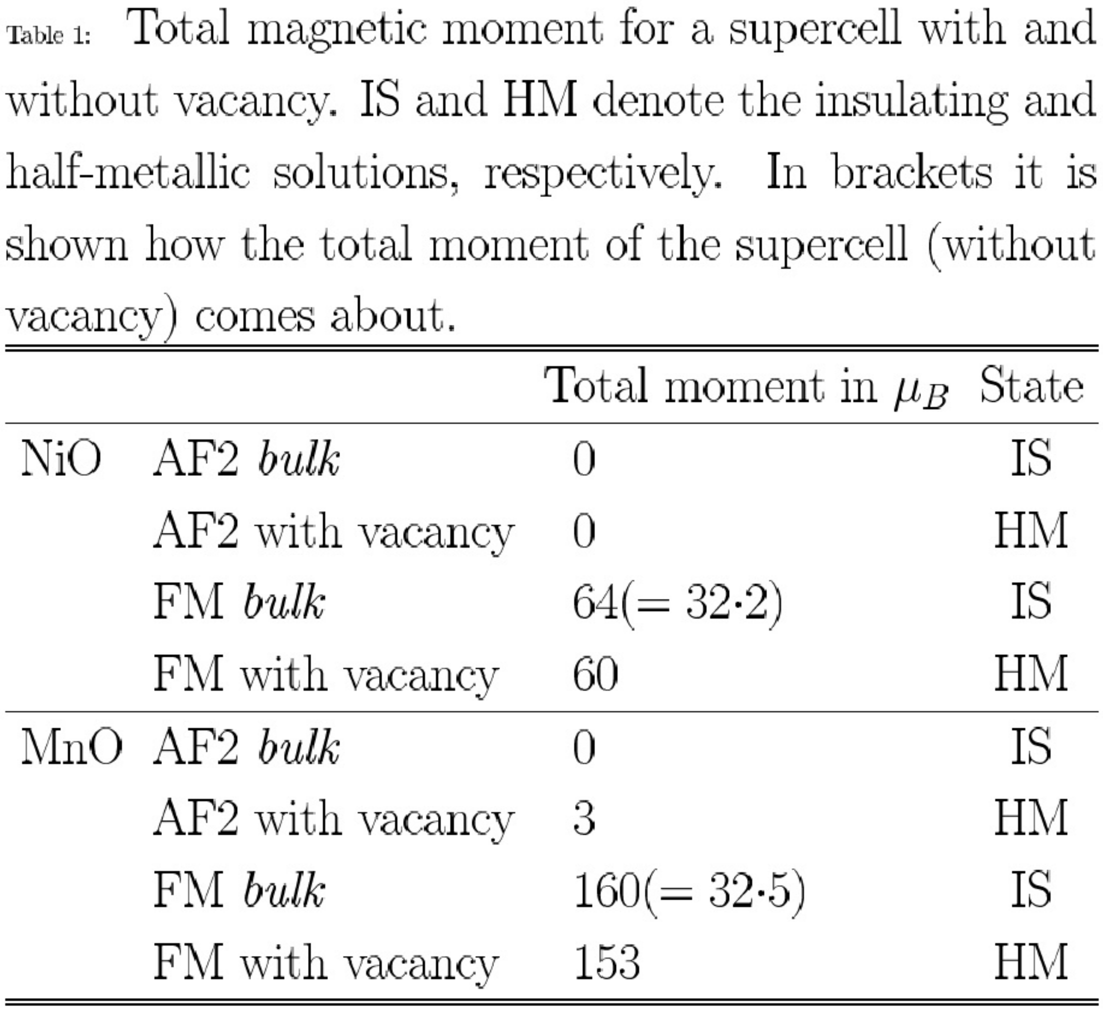

Table 1: Total magnetic moment for a supercell with and without vacancy. IS and HM denote the insulating and half-metallic solutions, respectively. In brackets it is shown how the total moment of the supercell (without vacancy) comes about.

		Total moment in μ_B	State
NiO	AF2 *bulk*	0	IS
	AF2 with vacancy	0	HM
	FM *bulk*	$64 (= 32 \cdot 2)$	IS
	FM with vacancy	60	HM
MnO	AF2 *bulk*	0	IS
	AF2 with vacancy	3	HM
	FM *bulk*	$160 (= 32 \cdot 5)$	IS
	FM with vacancy	153	HM

Conclusions

- Fe3O4: *the charge ordered insulating phase is not the lowest energy solution for either cubic or orthorhombic, low temperature, structure.*
- *SIC-LSD leads to large Mo spin moment in double perovskites that is always anti-parallel with respect to Fe spin moment.* Fe^{3+} *is the lowest energy solution.*
- *3% TM vacancy doping induced transition from insulating to half-metallic behaviour with NiO becoming HMAF. More studies are necessary .*

Acknowledgements

W.M. Temmerman *(Daresbury)*
D. Ködderitzsch (Halle)
G.M. Stocks (Oak Ridge)
L. Petit (Aarhus)
A. Svane (Aarhus)
H. Winter (Karlsruhe)

Thanks to:

P.H. Dederichs (Jülich)
T. Saha-Dasgupta (Calcutta)
V. Antonov (Kiev)